This article was downloaded by: *[United States Naval Academy]*
On: *21 January 2009*
Access details: *Access Details: [subscription number 789040243]*
Publisher *Taylor & Francis*
Informa Ltd Registered in England and Wales Registered Number: 1072954 Registered office: Mortimer House, 37-41 Mortimer Street, London W1T 3JH, UK

Biofouling
Publication details, including instructions for authors and subscription information:
http://www.informaworld.com/smpp/title~content=t713454511

The influence of biofilms on skin friction drag

Michael P. Schultz [ab]; Geoffrey W. Swain [c]
[a] Division of Engineering R&D, Harbor Branch Oceanographic Institution, Fort Pierce, FL, USA [b] Ocean Engineering Program, Florida Institute of Technology, Melbourne, FL, USA [c] Department of Mechanical Engineering, United States Naval Academy, Annapolis, MD, USA

First Published on: 01 January 2000

To cite this Article Schultz, Michael P. and Swain, Geoffrey W.(2000)'The influence of biofilms on skin friction drag',Biofouling,15:1,129 — 139

To link to this Article: DOI: 10.1080/08927010009386304

URL: http://dx.doi.org/10.1080/08927010009386304

PLEASE SCROLL DOWN FOR ARTICLE

Full terms and conditions of use: http://www.informaworld.com/terms-and-conditions-of-access.pdf

This article may be used for research, teaching and private study purposes. Any substantial or systematic reproduction, re-distribution, re-selling, loan or sub-licensing, systematic supply or distribution in any form to anyone is expressly forbidden.

The publisher does not give any warranty express or implied or make any representation that the contents will be complete or accurate or up to date. The accuracy of any instructions, formulae and drug doses should be independently verified with primary sources. The publisher shall not be liable for any loss, actions, claims, proceedings, demand or costs or damages whatsoever or howsoever caused arising directly or indirectly in connection with or arising out of the use of this material.

Biofouling, 2000, Vol 15(1–3), pp 129–139
Reprints available directly from the publisher
Photocopying permitted by license only

© 2000 OPA (Overseas Publishers Association) N.V.
Published by license under
the Harwood Academic Publishers imprint,
part of The Gordon and Breach Publishing Group.
Printed in Singapore.

The Influence of Biofilms on Skin Friction Drag

MICHAEL P SCHULTZ[1,*] and GEOFFREY W SWAIN[2]

[1]*Division of Engineering R&D, Harbor Branch Oceanographic Institution, 5600 US 1 North, Fort Pierce, FL 34946, USA;* [2]*Ocean Engineering Program, Florida Institute of Technology, 150 West University Boulevard, Melbourne, FL 32901, USA*

(Received 15 June 1999; in final form 16 September 1999)

The contribution of biofilms to skin friction drag is not clearly defined, and as regulations continue to restrict the use of biocides in antifouling paints, they are likely to form a greater presence on ship hulls. This paper reviews the flow regime around a ship's hull, the basics of boundary layer structure, and the effects of rigid surface roughness on drag. A review of experimental studies of biofilms in turbulent shear flows at laboratory and ship-scale is made. The consensus of these studies shows that biofilms increase skin friction drag. Some measurements carried out in turbulent boundary layer flow using a two-component, laser Doppler velocimeter (LDV) are also presented. These results indicate an increase in skin friction for biofilms that is dependent on composition as well as thickness.

Keywords: drag; biofilm; skin friction; turbulent boundary layer

INTRODUCTION

Marine structures, even those protected by antifouling (AF) systems, are usually colonized by microfouling organisms that produce a biofilm. The effect of these films on frictional resistance is of practical importance in predicting the performance of marine vehicles. The complex nature of biofilms, including their irregular topography, compliance, and their ability to produce extracellular polymeric substances (EPS) make flows over them difficult to predict. In this paper, the basics of turbulent boundary layers and skin friction drag are discussed. The effects of surface roughness on the boundary layer and on drag are presented. The complexities of the biofilm as a class of surface roughness are addressed. Results from the authors' research as well as those from previous investigations are given.

BACKGROUND

Flow Around a Ship

In order to assess the effect of biofilms on frictional resistance, a basic understanding of the flow regime around a ship's hull is required (Figure 1). Some of the more salient features include the boundary layer and the points of transition and separation. The boundary layer is the area closest to the hull in which the fluid is impeded as a result of its viscosity. Prandtl first

*Corresponding author. Present address: Department of Mechanical Engineering, United States Naval Academy, Annapolis, MD 21402, USA; fax: (410)293-3041; email: mschultz@nadn.navy.mil

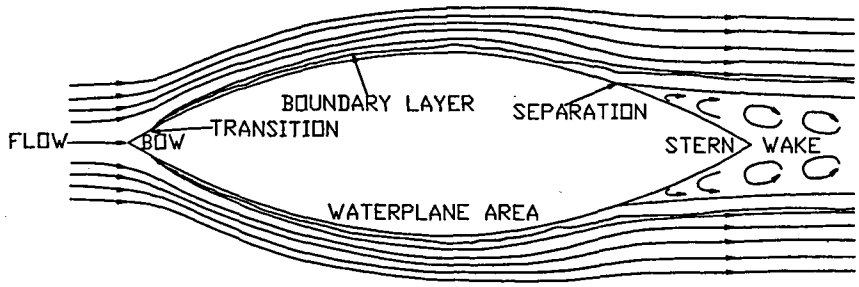

FIGURE 1 Schematic of the flow regime along a ship (adapted from Gillmer & Johnson, 1982).

introduced the boundary layer concept in 1904 (Schlichting, 1979). He reasoned that, in fluid flow around an object, the velocity at the surface of an object is zero (no-slip condition), and at some distance away from the object, the velocity is the freestream value. In the layer between the two, there must exist a velocity gradient. He called this the boundary layer. The thickness of the boundary layer, δ, increases down the length of the hull and may reach a meter or more in thickness on a large ship.

In a boundary layer developing over a surface, the flow remains laminar for a distance downstream. After some development, instabilities arise, and the flow begins to transition to turbulence. The transition process is dependent primarily on the non-dimensional quantity known as the Reynolds number, Re. It is defined as follows (Eqn 1):

$$\begin{aligned} \mathrm{Re} = {} & [(\text{freestream fluid velocity}) \\ & \times (\text{downstream distance})] \\ & /\text{kinematic viscosity of the fluid} \\ \Rightarrow \mathrm{Re}_x = {} & \frac{U_e x}{\nu} \end{aligned} \tag{1}$$

Transition occurs at a Reynolds number of approximately 1×10^6 on a smooth flat plate. For a ship moving at $10\,\mathrm{ms}^{-1}$, transition takes place at about 0.1 m downstream of the bow. Since a turbulent boundary layer covers the majority of the hull, it will be the focus of this discussion. Further downstream, the boundary layer may detach from the hull, and flow reversal may occur. This is termed the point of separation. Separation leads to an area of low pressure around the stern that increases the form drag on the hull.

Turbulent Boundary Layer Basics

Turbulent boundary layers are marked by velocity fluctuations in all three directions even though the mean flow may be steady. For this reason, the velocity at an instant in time may be expressed as the mean plus a fluctuating component. This is called Reynolds decomposition (Eqn 2).

$$\begin{aligned} u &= U + u' \\ v &= V + v' \\ w &= W + w' \end{aligned} \tag{2}$$

The turbulent boundary layer is considered to consist of several regions (Figure 2). These include the viscous sublayer, the log-law region, and the outer region (Ligrani, 1989). The viscous sublayer and the log-law region comprise the inner layer region. This region consists of the innermost 10–20% of the turbulent boundary layer (*i.e.* $y/\delta = 0$ to 0.1–0.2). Although the inner region is relatively thin, about 70% of the velocity variation occurs there. The local mean velocity in this region is a function of only the wall shear stress, the fluid density, kinematic viscosity, and distance from the wall. Therefore, the fluid velocity may be expressed in the following functional form, called

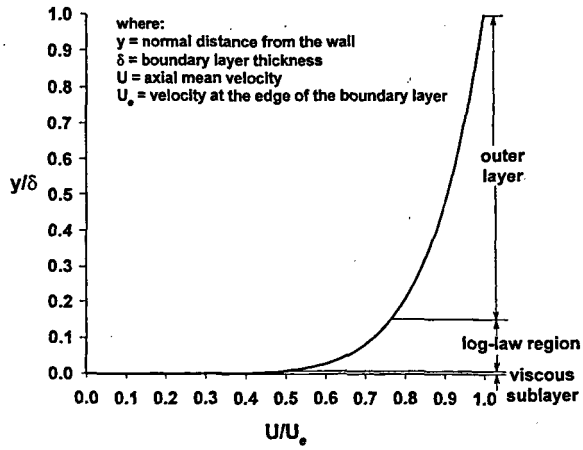

FIGURE 2 Turbulent boundary layer mean velocity profile.

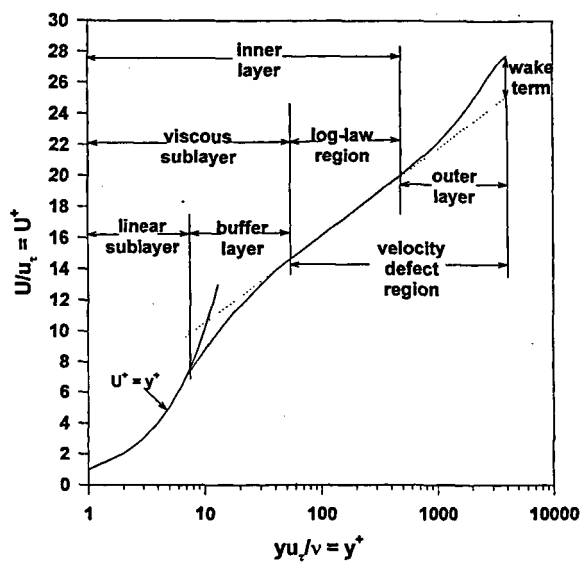

FIGURE 3 Law of the wall plot for a turbulent boundary layer (adapted from Bradshaw, 1976).

the law of the wall (Eqn 3).

$$\frac{U}{u_\tau} = f\left[\frac{yu_\tau}{\nu}\right] \Rightarrow U^+ = f[y^+] \tag{3}$$

Mean velocity profiles are frequently presented in this functional form. Figure 3 shows the law of the wall plot for a smooth wall, turbulent boundary layer.

The viscous sublayer is made up of two parts, *viz.* the linear sublayer and the buffer layer. The linear sublayer lies in a thin zone closest to the boundary, and it extends out only to about $y^+ = 7$. In this region the velocity profile is linear and is given by Eqn 4.

$$U^+ = y^+ \tag{4}$$

Across the linear sublayer, the total shear stress is almost constant and equal to the wall shear stress, τ_0. The wall shear stress is often normalized with the dynamic pressure to form the skin friction coefficient, C_f (Eqn 5).

$$C_f = \frac{\tau_0}{\frac{1}{2}\rho U_e^2} \tag{5}$$

The buffer layer occurs from about $7 < y^+ < 40$, and in this layer, the velocity profile departs from linearity. This is the region of the highest turbulence. The flow just outside the viscous sublayer is also highly turbulent in nature. In this region ($40 < y^+$ and $y/\delta < 0.15$), the total shear stress is constant and is mainly due to the fluctuating velocity components in the flow. This turbulent stress is often referred to as Reynolds stress. This region of the flow is called the log-law region, and the velocity distribution is given by Eqn 6.

$$U^+ = A\log(y^+) + B \tag{6}$$

The remaining 80–90% of the boundary layer is termed the outer layer. Figure 3 shows that at higher values of y^+ the velocity profile begins to rise above that predicted by the log-law. This is termed the wake. In the outer layer the total shear stress is not constant, and it decays to zero as the edge of the boundary layer is approached.

In the boundary layer, the total shear stress, τ, is made up of both viscous and turbulent stresses. The total shear stress may be written as Eqn 7. The shear stress profile is shown in Figure 4.

$$\begin{aligned} \text{Total shear stress} &= \text{viscous shear stress} \\ &\quad + \text{turbulent shear stress} \\ \tau &= \mu\frac{\partial U}{\partial y} - \rho\overline{u'v'} \end{aligned} \tag{7}$$

(Note that $-\rho\overline{u'v'}$ is a positive contribution to the total shear stress.)

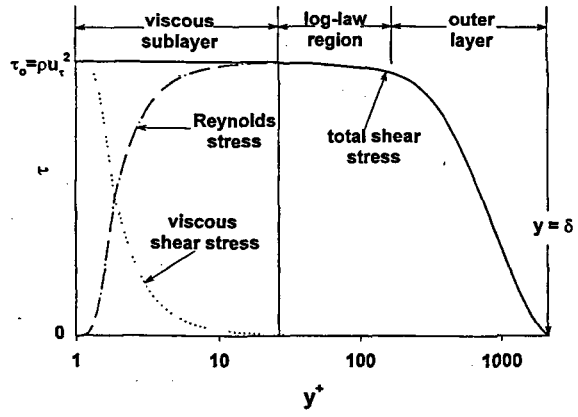

FIGURE 4 Turbulent boundary shear stress profile (adapted from Ligrani, 1989).

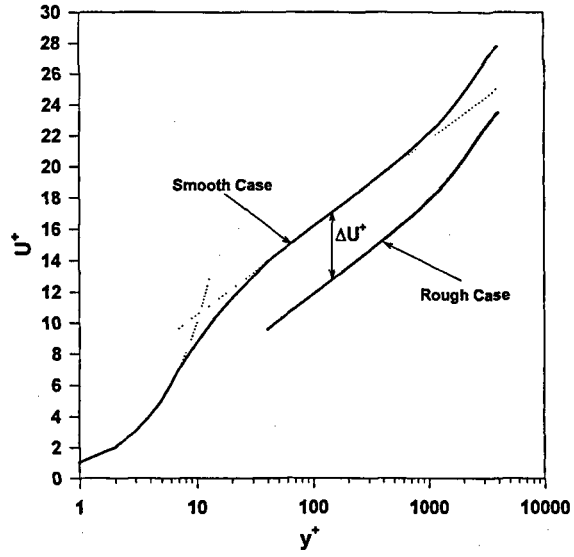

FIGURE 5 The effect of roughness on the law of the wall (adapted from Hama, 1954).

Effects of Rigid Surface Roughness

Wall roughness leads to increased turbulence and fluid mixing in the boundary layer. This manifests itself as increased turbulent and wall shear stress. Most surface roughness is said to be *k*-type, *i.e.* the change in skin friction scales in some fashion on *k*, the roughness height (Perry *et al.*, 1969). A simple example of such a surface is a monodispere, closely-packed sand roughness. Three distinct flow regimes can be identified for this type of roughness. These are the hydrodynamically smooth regime, the intermediate regime, and the fully rough regime. The degree to which the roughness has an effect on wall shear stress and the turbulent boundary layer is characterized by a parameter called the roughness Reynolds number, $k^+ = ku_\tau/\nu$.

In the hydrodynamically smooth regime ($k^+ < 5$), the roughness elements are sufficiently small to be completely submerged in the linear sublayer. In this case, the skin friction is equal to a smooth surface, and the near-wall shear stress is dominated by the viscous component. In the intermediate flow regime ($5 < k^+ < 70$), skin friction is increased relative to the smooth wall value. The near-wall shear stress is composed of both viscous and turbulent components. In the fully rough flow regime ($k^+ > 70$), the linear sublayer is completely destroyed, and the near-wall shear stress is dominated by the turbulent component. In flows around most marine vehicles, hydrodynamically smooth conditions do not prevail, as small surface imperfections have increasing influence at higher velocities. It is the intermediate flow regime that is of the greatest practical importance in full-scale ship conditions. Ships rarely operate in the rough regime because of the large drag penalties, and hydrodynamically smooth surfaces are difficult to achieve and maintain (Grigson, 1985).

The effect of roughness can be seen in the mean velocity profile also. It results in a loss in momentum in the inner region that is characterized by a downward shift in the log-law. This shift is called the roughness function, ΔU^+. It is illustrated in Figure 5 and Eqn 8.

$$\Delta U^+ = A \log[y^+] + B - \Delta U^+ \qquad (8)$$

One of the elusive goals of experimentalists in fluid mechanics is to develop a universal relationship between the physical measures of an arbitrary surface and its roughness function.

Colebrook and White (1937) and Colebrook (1939) showed that the roughness functions of some engineering surfaces could be expressed in the following form (Eqn 9):

$$\Delta U^+ = A \log[1 + k^+] \tag{9}$$

Granville (1987), Townsin and Dey (1990), and Grigson (1992) have shown that for irregular roughness, such as found on a newly painted ship, the roughness texture is also an important scaling parameter. Townsin and Dey (1990) proposed a "Colebrook type" roughness function that also incorporated surface texture. Their relationship was developed for ship hull surfaces and was based on measurements of the roughness profile (Eqn 10).

$$\Delta U^+ = A \log\left[1 + 0.18\frac{hu_\tau}{\nu}\right] \tag{10}$$

The incorporation of a physical measure of the texture of a rough surface into Eqn 11 leads to improved agreement with experimental results, but, a significant scatter in the results still exist. Grigson (1992) stated that the texture of a surface is difficult to characterize without experimental flow measurements. For this reason, he proposed that rough surfaces should be analyzed in laboratory hydrodynamic tests. The results of these tests then should be fit to Eqn 11.

$$\Delta U^+ = A \log\left[1 + \sum_1^n A_n\left(\frac{ku_\tau}{T\nu}\right)^n\right] \tag{11}$$

Grigson found that a power series of order three was generally sufficient to explain most of the variance in the results, and no surface that he studied required higher than a sixth order power series. While Eqn 11 may accurately define the roughness function, it requires laboratory scale hydrodynamic testing of the surface. At present, reliable prediction of the skin friction drag of an arbitrary rough surface based solely on measurements of its surface profile is elusive.

BIOFILM COMPLEXITIES

The roughness types discussed in the previous section were fairly uniform and rigid. Marine biofilms are neither. They consist of microbial cells that attach to a substrate and proceed to grow, reproduce, and synthesize extracellular polymeric substances (EPS) dominated by polysaccharides (Christensen & Characklis, 1990). They range from fairly uniform to patchy in coverage and may trap considerable amounts of inorganic particles such as silt and clay minerals. The scale of the component organisms ranges from bacteria (micrometres) to filamentous algae (centimeters). The complexity of the marine biofilm is obvious. A surface coated with a heterogeneous compliant biotic polymer with entrapped organisms is very different and much more complex than a homogeneous sand roughness.

Two of the biofilm characteristics mentioned have been previously exploited to reduce drag, *viz.* compliance and polymers. Drag reduction due to surface compliance is largely a result of delaying transition by damping turbulent instabilities, although some recent results show modest reductions in turbulent boundary layers (Gad-el-Hak, 1998). This does not appear to be a practical drag reduction mechanism for a biofilm-coated hull. Since the flow on a ship becomes turbulent very near the bow, increasing the Reynolds number for transition by a factor of ten would do little to reduce the overall skin friction drag. Solutions of polymers have also been shown to produce drag reduction (Berman, 1978; Harder & Tiederman, 1991). Two categories of polymers have been shown to be effective. These are the spherical random coil type and the extended polyelectrolyte type. In order for a polymer to be effective, it must have a molecular weight of $> 10^5$ (Berman, 1978). The polymer must also be present in the buffer region of the boundary layer in sufficient concentration to reduce drag (Harder & Tiederman, 1991). Polymers tethered to the surface are ineffective. It is not known if polymers found in biofilm EPS are

effective in drag reduction, but even if they are, it seems unlikely that biofilm organisms would be able to produce these polymers in sufficient quantity to reduce drag on a ship over a significant period of time.

EXPERIMENTAL RESULTS

A great deal of research has been devoted to studying the effects of fouling on drag. Much of this has focused on macrofouling. However, several studies have been devoted to biofilms. McEntee (1915) asserted that biofilms increased the resistance of full-scale ships 0.5% d^{-1} while they were moored pierside. Experiments at Langley Field on towed plates also showed that slime films increase skin friction (Benson *et al.*, 1938). In resistance measurements on the *Lucy Ashton*, skin friction increased about 5% after the vessel remained pierside for 40 d (Denny, 1951). The increase was attributed to a thin coat of slime and deterioration of the bituminous aluminum paint on her hull. Watanabe *et al.* (1969) carried out experiments on slime coated concentric cylinders, rotating disks, and a model ship. From extrapolation of these results, they predicted an increase in full-scale ship resistance of 9–10% due to slime fouling.

An investigation of the effects of a microbial biofilm on turbulent pipe flow was carried out by Picologlou *et al.* (1980). A strong positive correlation between the biofilm thickness and the pipe friction factor was observed. They also noted that the viscoelastic character of the biofilm combined with its filamentous nature appeared to cause additional energy dissipation mechanisms that caused higher frictional resistance than a rigid surface roughness of similar height. Lewkowicz and Das (1986) used uniformly distributed nylon tufts attached to a rough flat plate in order to model a marine slime growth. They found that C_f was an average of 18% higher for the model slime film with a background roughness than for the background roughness alone. Loeb *et al.* (1984) measured the influence of microbial biofilms on the hydrodynamic drag of rotating discs. Their data showed an increase in frictional resistance of 10% to 20% due to slime films. Since it was hypothesized that a thin slime film might reduce the drag of a rough surface by effectively smoothing it, pre-roughened discs were also tested before and after biofilm formation. An increase in frictional drag of 10% was measured for the fouled, rough disc.

Lewthwaite *et al.* (1985) conducted an experiment in which mean boundary layer velocity profiles were measured on a 23 m fleet tender. An 83% increase in C_f and a 15% reduction in ship speed were noted over a 2 year exposure. No quantitative measurements were made on the fouling settlement except to note that when the vessel was drydocked, it was covered with a dense slime film $\sim$1 mm thick. When the hull was cleaned and returned to the water, measurements confirmed that C_f returned approximately to its clean hull value.

Haslbeck & Bohlander (1992) carried out a full-scale trial on a Knox class frigate instrumented to measure shaft horsepower and ship speed. The ship, which was coated with an ablative antifouling paint containing both cuprous oxide and tributyltin oxide, had been stationed in Pearl Harbor, Hawaii for 22 months. An initial hull inspection by divers indicated the presence of a microbial biofilm and little macrofouling. After removing the biofilm by underwater cleaning, there was an 18% decrease in the required shaft horsepower to propel the ship at same speed.

Recently, the authors made measurements of the mean and fluctuating velocity statistics in turbulent boundary layer flows over marine biofilms (Schultz, 1998; Schultz & Swain, 1999). The study was conducted in a recirculating water tunnel facility using a two-component laser Doppler velocimeter (LDV). Measurements were made at freestream velocities of 1.50, 2.25, and 3.00 ms^{-1} on two smooth surfaces and three biofilms. All of the test surfaces were fabricated from cast acrylic sheet. Visual assessment as well as thickness

TABLE I Biofilm coverage and constituents before and after hydrodynamic testing

Specimen	Total % fouling cover	Constituents and their % cover
F1 before	97	Slime 97% (light to medium density film); biofilm thickness 350 ± 69 μm
F1 after	70	Slime 70% (very light density film); cyanobacteria (*Anabaena oscillarioides*) and marine diatoms (dominated by *Melosira* spp.); biofilm thickness* 74 ± 46 μm
F2 before	98	Slime 94% (medium density film); filamentous green algae 4%; biofilm thickness 160 ± 41 μm
F2 after	91	Slime 90% (medium density film); filamentous green algae 1%; green algae (*Enteromorpha* spp.) and marine diatoms (dominated by *Melosira* spp. and *Thallasiothrix* spp.); biofilm thickness 130 ± 27 μm
F3 before	95	Slime 70% (medium density film); filamentous green algae 25%; biofilm thickness 310 ± 100 μm
F3 after	82	Slime 70% (medium density film); filamentous green algae 12%; (*Enteromorpha* spp.); biofilm thickness 340 ± 150 μm

*Most of biofilm F1 remained attached until the highest freestream velocity

measurements using a wet film thickness gauge were made on the fouling both before and after testing. These results are shown in Table I. Further details of the experimental setup and data analysis techniques are given in Schultz (1998).

A result illustrated in Table I is the difference in tenacity of the various biofilm components. Much of biofilm F1, dominated by cyanobacteria, was removed at the highest freestream velocity. The other biofilms were affected to a lesser degree. The wall shear stress, τ_0, for F1 at $U_e = 3.00\,\mathrm{ms}^{-1}$ was ~ 18 Pa. This provides an indication of the shear stress required to remove cyanobacteria from an acrylic substrate.

Figure 6 shows C_f *vs* the momentum thickness Reynolds number for the smooth and fouled surfaces. Biofilm specimens F1, F2, and F3 have an increase in C_f of 8% to 130%, 3% to 70%, and 11% to 370%, respectively, compared to the smooth plates. The average increase was 70% for F1, 30% for F2, and 190% for F3. A lot of scatter in the results for the fouled specimens can be seen. This is likely to be the result of streamwise heterogeneity in the biofilm. A Kruskal-Wallis ANOVA on ranks and Student-Newman-Keuls pairwise comparisons at $\alpha = 0.05$ (Sokal & Rohfl, 1981) indicate a significant difference between all the smooth surfaces and the biofilms with the exception of the two smooth controls and F1 *vs* F2. It is of note that F3, dominated by filamentous algae, had a significantly higher skin friction than F1 despite their similar mean thickness measured before testing. These results indicate that biofilm composition is an important factor in determining skin friction, *i.e.* filamentous biofilms lead to greater increases in skin friction than non-filamentous films of similar thickness.

Figure 7 illustrates the effect of the biofilms on the mean velocity profile in the boundary layer. A downward shift in the log-law for all of the biofilm profiles is seen. The magnitude of the shift varied considerably, however. This can be seen in the scatter of the roughness functions shown in Figure 8, which illustrates the rapid streamwise changes in the boundary layer due to biofilm heterogeneity discussed previously. Similar variability was observed in the turbulent structure, because abrupt changes in the surface roughness does not allow a self-similar or equilibrium boundary layer to develop as it does on a smooth or uniformly rough surface.

None of the biofilms showed good collapse to a Nikuradse or Colebrook roughness function. The scaling length used in Figure 8 was the mean biofilm height before testing. Attempts to use other scaling parameters did not lead to any better

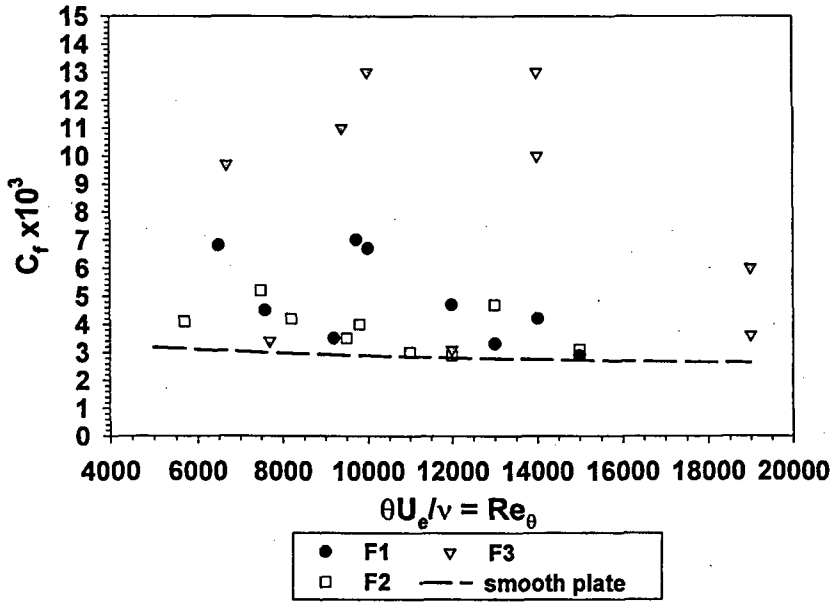

FIGURE 6 The effect of biofilms on the skin friction coefficient (Schultz & Swain, 1999).

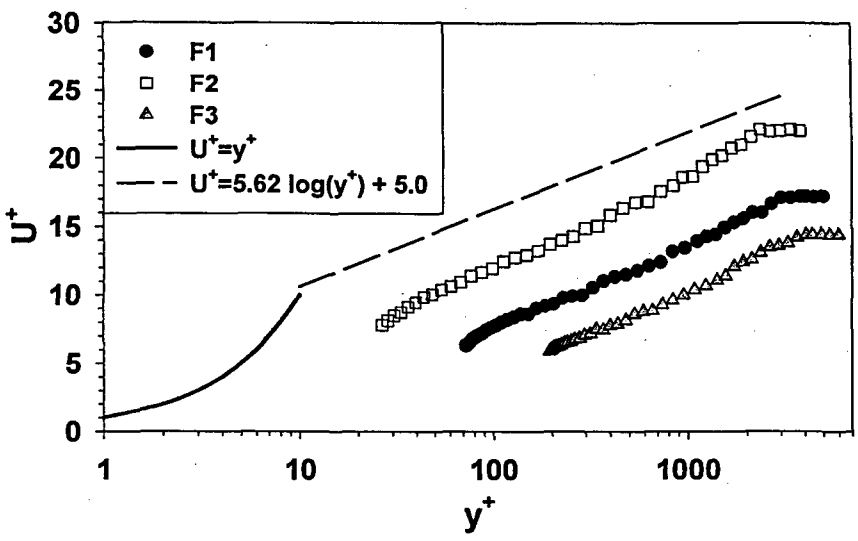

FIGURE 7 The effect of biofilms on the law of the wall (Schultz & Swain, 1999).

collapse of the data. It is likely that parameters such as the shear modulus of the biofilm are also important. In practice, however, they are difficult to measure. It is the authors' opinion that techniques such as laser interferometry could be useful in documenting the biofilm topography while under flow. It seems likely that statistical analysis of the biofilm surface profile under flow would lead to more meaningful roughness scaling parameters than the wet film thickness measured in air. More research needs to be carried out in this area if the physical measurements of a biofilm are to be accurately related to its skin friction drag.

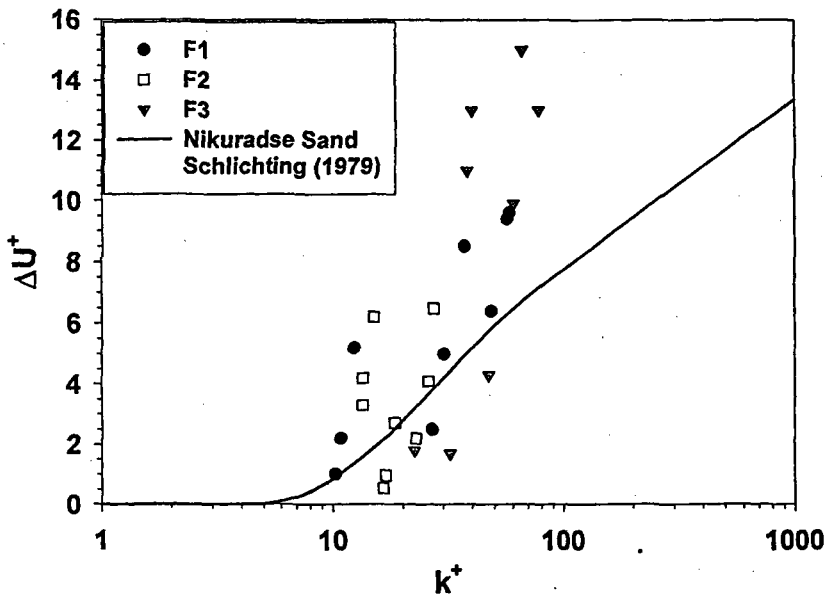

FIGURE 8 Biofilm roughness functions (Schultz & Swain, 1999).

The results show that the magnitude of the turbulent fluctuations and the Reynolds shear stress increased for the biofilm surfaces over the range $0.2 \leq y/\delta \leq 0.5$. The increase in the axial turbulence component was greater than in the wall-normal component for all three biofilms. The average increase in the axial turbulence component was 29%, 23%, and 52%, for F1, F2, F3, respectively. The average increase in the wall-normal turbulence was 25%, 19%, and 45%, for F1, F2, F3, respectively. The results were variable when the turbulence quantities were normalized with the friction velocity (Schultz & Swain, 1999).

SUMMARY

Experimental studies in the laboratory and full-scale sea trials show that biofilms can significantly increase skin friction drag on marine vehicles. Both biofilm thickness and composition are important in determining the increase in the wall shear stress. Biofilms alter both the mean and turbulent velocity structure in the boundary layer. Rapid streamwise changes may occur in the mean and turbulence profiles as a result of biofilm heterogeneity. Biofilms should be considered when addressing the need for hull cleaning. Further research must be carried out in order to identify scaling parameters that allow accurate prediction of skin friction drag based on physical measurements of the biofilm.

Acknowledgements

The authors would like to thank the Office of Naval Research (grant # N00014-91-J-1465) and the Environmental Security and Technology Certification Program for their support of this research.

NOMENCLATURE

A	log-law slope = 5.62 (Coles, 1969)
B	log-law intercept = 5.0 (Coles, 1969)
C_f	skin friction coefficient = $\tau_0/(0.5\rho U_e^2)$

h	Townsin's roughness height parameter $= (\alpha m_0 m_2)^{1/2}$
k	roughness height
k^+	roughness Reynolds number $= ku_\tau/\nu$
m_0, m_2, m_4	the 0th, 2nd, and 4th spectral moments of the roughness profile
Re_x	Reynolds number $= xU_e/\nu$
Re_θ	momentum thickness Reynolds number $= \theta U_e/\nu$
T	roughness texture parameter
U_e	mean axial velocity at boundary layer edge
U^+	U/u_τ
u_τ	friction velocity $= (\tau_0/\rho)^{1/2}$
U, V, W	mean axial, wall-normal, and transverse velocities
u, v, w	instantaneous axial, wall-normal, and transverse velocities
u', v', w'	fluctuating axial, wall-normal, and transverse velocities
$\overline{u'v'}$	cross-correlation of the axial and wall-normal velocity fluctuation
x, y, z	axial, wall-normal, and transverse directions
y^+	yu_τ/ν
α	$(m_0 m_4)m_2$
δ	boundary layer thickness
ΔU^+	roughness function
μ	absolute viscosity of the fluid
ν	kinematic viscosity of the fluid
ρ	density of the fluid
θ	momentum thickness $= \int_0^\delta (U/U_e)(1-(U/U_e))\,\mathrm{d}y$
τ	shear stress
τ_0	wall shear stress

References

Benson J M, Ebert J W, Beery T D (1938) Investigation in the NACA tank of the effect of immersion in salt water on the resistance of plates coated with different shipbottom paints. NACA Memorandum Report C&R C-S19-1(3)

Berman N S (1978) Drag reduction by polymers. *Annu Rev Fluid Mech* **10**: 47–64

Bradshaw P (1976) Introduction. In: Bradshaw P (ed) *Turbulence*. Springer-Verlag, Berlin

Christensen B E, Characklis W G (1990) Physical and chemical properties of biofilms. In: Characklis W G, Marshall K C (eds) *Biofilms*. John Wiley and Sons, New York, pp 93–130

Colebrook C F (1939) Turbulent flow in pipes, with particular reference to the transition region between smooth and rough pipe laws. *J Civil Eng* **11**: 133–157

Colebrook C F, White C M (1937) Experiments with fluid resistance in roughened pipes. *Proc R Soc* **161A**: 376–381

Coles D (1969) The young person's guide to the data. In: Coles D E, Hirst E A (eds) *Computation of Turbulent Boundary Layers*. 1968 AFOSR-IFP Stanford Conference 2, Thermosciences Division, Stanford University, pp 1–45

Denny M E (1951) B.S.R.A. resistance experiments on the "Lucy Ashton": Part I full – scale measurements. *Trans RINA* **93**: 40–57

Gad-el-Hak M (1998) Compliant surfaces: the simpler alternative. *Proc ONR Int Symp Seawater Drag Reduction*, Newport, pp 197–204

Gillmer T C, Johnson B (1982) *Introduction to Naval Architecture*. Naval Academy Press, Annapolis

Granville P S (1987) Three indirect methods for the drag characterization of arbitrarily rough surfaces on flat plates. *J Ship Res* **31**: 70–77

Grigson C W B (1985) Velocity loss functions of rough surfaces in intermediate flow. *Proc 2nd Int SSPA Symp Ship Viscous Resistance*, Goteborg, 18:1–18:25

Grigson C W B (1992) Drag losses of new ships caused by hull finish. *J Ship Res* **36**: 182–196

Hama F R (1954) Boundary-layer characteristics for rough and smooth surfaces. *Trans SNAME* **62**: 333–351

Harder K J, Tiederman W G (1991) Drag reduction and turbulent structure in two-dimensional channel flows. *Philos Trans R Soc Lond* **336**: 19–34

Haslbeck E G, Bohlander G (1992) Microbial biofilm effects on drag-lab and field. *Proc 1992 SNAME Ship Production Symp*

Lewkowicz A K, Das D K (1986) Turbulent boundary layers on rough surfaces with and without a pliable overlayer: a simulation of marine fouling. *Int Shipbuilding Prog* **33**: 174–186

Lewthwaite J C, Molland A F, Thomas K W (1985) An investigation into the variation of ship skin frictional resistance with fouling. *Trans RINA* **127**: 269–284

Ligrani P M (1989) Structure of turbulent boundary layers. In: Cheremisinoff N P (ed) *Encyclopedia of Fluid Mechanics*. Gulf Publishing, pp 112–189

Loeb G I, Laster D, Gracik T (1984) The influence of microbial fouling films on hydrodynamic drag of rotating discs. In: Costlow J D, Tipper R (eds) *Marine Biodeterioration: an Interdisciplinary Study*. Naval Institute Press, Annapolis, MD, pp 88–94

McEntee W (1915) Variation of frictional resistance of ships with condition of wetted surface. *Trans Soc Nav Arch Mar Eng* **24**: 37–42

Perry A E, Schofield W H, Joubert P N (1969) Rough-wall turbulent boundary layers. *J Fluid Mech* **17**: 193–211

Picologlou B F, Zelver N, Characklis W G (1980) Biofilm growth and hydraulic performance. *ASCE J Hydraulics Div* **HY5**: 733–746

Schlichting H (1979) *Boundary-Layer Theory*. 7th Edition, McGraw-Hill, New York

Schultz M P (1998) The effect of biofilms on turbulent boundary layer structure. PhD Dissertation, Florida Institute of Technology, Melbourne, FL

Schultz M P, Swain G W (1999) The effect of biofilms on turbulent boundary layers. *ASME J Fluids Eng* **121**: 733–746

Sokal R R, Rohfl F J (1981) *Biometry: The Principles and Practice of Statistics in Biological Research.* W H Freeman, San Francisco

Townsin R L, Dey S K (1990) The correlation of roughness drag with surface characteristics. *Proc RINA Int Workshop Marine Roughness Drag*

Watanabe S, Nagamatsu N, Yokoo K, Kawakami Y (1969) The augmentation in frictional resistance due to slime. *J Kansai Soc Nav Arch* **131**: 45–51